PERGAMON

International Journal of Solids and Structures 39 (2002) 4407–4420

INTERNATIONAL JOURNAL OF SOLIDS and STRUCTURES

www.elsevier.com/locate/ijsolstr

The influence of an edge radius on the local stress field at the edge of a complete fretting contact

A. Sackfield [1], A. Mugadu [2], D.A. Hills *

Department of Engineering Science, Oxford University, Parks Road, Oxford OX1 3PJ, UK

Received 18 December 2001; received in revised form 17 April 2002

Abstract

The state of stress adjacent to the corner of a complete or almost complete fretting contact pad is studied using the corresponding Muskhelishvili potentials. Three potential are employed; that for a semi-infinite rigid punch, that for a finite square-ended rigid punch, and that for a punch having a flat form with radiused corners. It is shown that the asymptotic stress field (the semi-infinite punch) matches the finite punch well over a large region. Further, the edge radius which can be tolerated, but still giving rise to a local stress field which can be approximated by the asymptotic solution is found. The implication of these results for the application of an asymptotic approach to the design of almost complete fretting contacts is described.

Keywords: Fretting fatigue; Complete contacts; Asymptotic solution

1. Introduction

The use of asymptotic analysis in quantifying fretting fatigue behaviour was pioneered by (Giannakopoulos et al., 1998). In that paper, he draws an analogy between the stress state existing at the corner of a square contact, and that present at the tip of a crack. This is attractive, because the formation of a crack may then be thought of as 'branching', which helps to remove some of the imponderables present in a crack initiation analysis. The principle difficulty is that a square-root singularity in the stress state exists only under rather restrictive conditions. A variation on this idea is to use frictional wedge asymptotics, as developed by Gdoutos and Theocaris (1975) and Comninou (1976) to quantify the local extended elastic stress state, within which a 'process zone' develops, whose characteristics are totally controlled by the singular field (Mugadu et al., 2002). This permits a generalised stress intensity factor to be developed, which controls the initiation environment. There are clearly very strong analogies, here, between the problem of initiation

* Corresponding author. Tel.: +44-1865-279800; fax: +44-1865-279802.
E-mail address: david.hills@eng.ox.ac.uk (D.A. Hills).
[1] Permanent address: Department of Mathematics, Nottingham Trent University, Burton Street, Nottingham, UK.
[2] Sponsored by the Rhodes Trust.

0020-7683/02/$ - see front matter
PII: S0020-7683(02)00337-2

at a complete fretting contact, and the extension of a crack in fracture mechanics. In each the process zone must be contained wholly within (well within) a singular elastic field, having a unique order of singularity, and a unique spatial distribution. This is the question of 'small scale yielding', and we have addressed this in relation to the contact problem in a recent article (Mugadu and Hills, 2002). A further feature required of the crack tip, before conventional fracture mechanics principles can be rigorously applied is that it must be 'sharp', for the singular stress state to apply. In the case of a crack this usually means that there must be no blunting caused by local plasticity, but in the case of a fretting contact, the problem is potentially more serious. All real contacts must be machined, and there must therefore, in reality, always be a local curvature. The question is; how big can that curvature be? A very straightforward and simplified way of answering this is to say that the radius of curvature must be small compared with the characteristic size of the process zone, but this is really only an estimation. A more rigorous approach is to examine the characteristic local stress field itself, and to see how closely the contact stress field adjacent to the edge of the contact for the 'flat-and-rounded' punch resembles the asymptotic stress appropriate to a semi-infinite square-ended punch, within the domain where the elastic stress field provides a controlling hinterland to the process zone. We have made a preliminary investigation using a comparison of the local pressure distributions (Navarro et al., submitted for publication), but here, a fuller approach using the complete local stress state is pursued.

2. Square-ended punch

Fig. 1 shows a rigid, square-ended punch, resting on an incompressible half-plane. The elastic constants are chosen in this way so that the presence of frictional shearing tractions does not modify the contact pressure distribution, which is given by

$$\frac{ap(x)}{P} = -\frac{1}{\pi\sqrt{1-(x/a)^2}}. \tag{1}$$

Here, P is the applied load and a the contact half width. The corresponding Muskhelishvili potential for the problem, with the punch now sliding, is

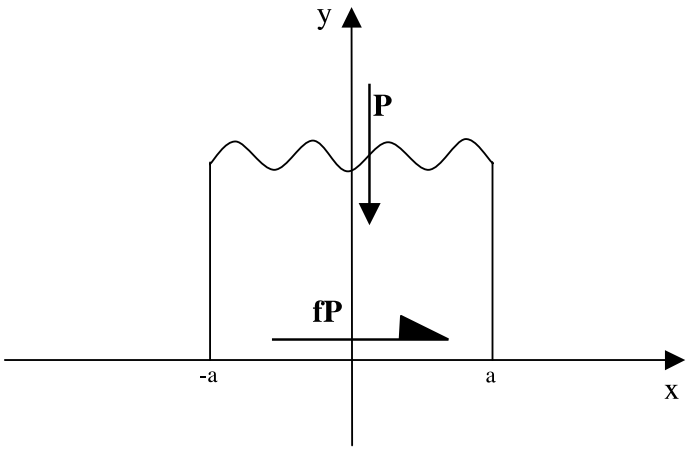

Fig. 1. Representation of a square-ended rigid punch on an incompressible half plane.

$$\frac{a\phi(z)}{P} = \frac{(\mathrm{i}+f)}{2\pi\sqrt{z^2-1}}, \tag{2}$$

where f is the coefficient of friction, $z = x/a + \mathrm{i}y/a$ and $\mathrm{i} = \sqrt{-1}$. Now move the origin to the left corner of the punch by the transformation $\eta = z + 1$, giving

$$\frac{a\phi(\eta)}{P} = \frac{(1-\mathrm{i}f)}{2\pi\sqrt{2\eta}}\left(1-\frac{\eta}{2}\right)^{-1/2} \tag{3}$$

and use the binomial theorem to extract the dominant term, so that, when $|\eta| \ll 1$

$$\frac{a\phi(\eta)}{P} \doteq \frac{(1-\mathrm{i}f)}{2\pi\sqrt{2\rho}}\exp(-\mathrm{i}\theta/2), \tag{4}$$

where $\eta = \rho\exp(\mathrm{i}\theta)$. This represents the behaviour of a semi-infinite punch, and is equivalent to the stress distribution given by a standard asymptotic analysis. It is therefore straightforward to discover explicitly the domain in which the singular term provides an accurate description of the local stress state. The stress field implied by the potential is characterised by two components, and it is possible to display these in various ways. Fig. 2(a) shows a plot of the normalised von Mises' parameter, $a\sqrt{J_2}_{\mathrm{asymp}}/P$, for a sample coefficient of friction, $f = 0.6$. The complete and asymptotic stress fields become identical as ρ becomes small (i.e. $\rho \ll 1$), and divergence occurs as the observation point moves away from the corner. The rate of divergence depends on the angle θ along which one moves away from the contact edge, and on the coefficient of friction, f. For a discrepancy between the full and asymptotic fields, $(\sqrt{J_2}_{\mathrm{full}} - \sqrt{J_2}_{\mathrm{asymp}})/\sqrt{J_2}_{\mathrm{full}}$, of less than 5%, the maximum value of ρ/a when $f = 0.6$, is about to 0.05, Fig. 2(b). From Fig. 2(a) this corresponds to a normalised load, $P/a\tau_{\mathrm{y}}$ of about 2.5, where τ_{y} is the yield stress in pure shear.

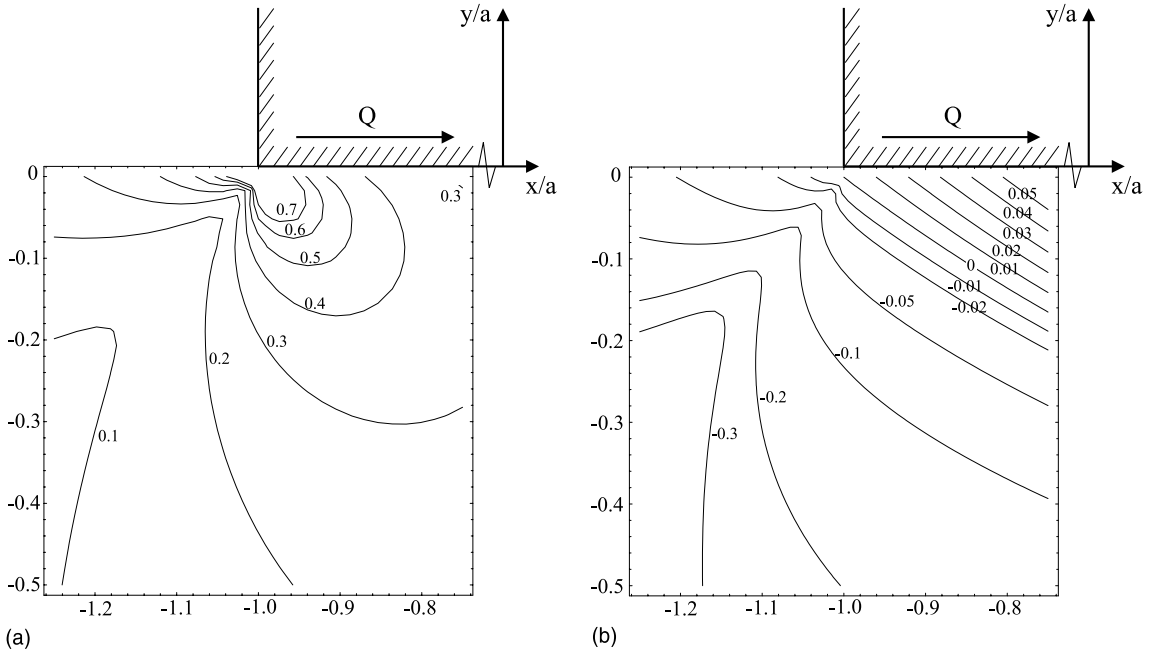

Fig. 2. (a) Plot showing the normalised von Mises' parameter, $a\sqrt{J_2}_{\mathrm{asymp}}/P$, for a rigid, square-ended semi-infinite punch, when $f = 0.6$. (b) Plot showing the discrepancy, $(a\sqrt{J_2}_{\mathrm{full}}/P - a\sqrt{J_2}_{\mathrm{asymp}}/P)/a\sqrt{J_2}_{\mathrm{full}}/P$, between the finite and semi-infinite square-ended punches at the contact edge for $f = 0.6$.

3. Flat-and-rounded punch

A new way of displaying the Muskhelishvili potential for this geometry, avoiding the need to use a series expansion is used. The procedure has been developed independently by Jäger (2002) to solve a wider range of contact geometries. Here, we use it merely as a direct method of obtaining a range of asymptotic solutions. Suppose that the contact problem itself has been solved, giving rise to a contact of half-width a, whilst the flat portion of the contact has a half-length ka (where $k < 1$), Fig. 3. Employing coordinates normalised with respect to the contact half-length, one form of the pressure distribution, which can be derived directly from Ciavarella et al. (1998) is

$$p(x) = -K\sqrt{1-x^2}\left[\int_{-1}^{-k} \frac{(k+t)\,\mathrm{d}t}{\sqrt{1-t^2}(t-x)} + \int_{k}^{1} \frac{(t-k)\,\mathrm{d}t}{\sqrt{1-t^2}(t-x)}\right], \quad |x| < 1, \tag{5}$$

where K is given by $E^*/2\pi R$ which, for the special case of two elastically similar bodies, becomes $E/4\pi R(1-\nu^2)$ with E denoting Young's Modulus, ν Poisson's ratio and R the radius of curvature of the corners of the punch. If the contact is in gross sliding, the Muskhelishvili potential is given by (Hills et al., 1993)

$$\Phi(z) = \frac{1-\mathrm{i}f}{2\pi\mathrm{i}} \int_{-1}^{1} \frac{p(x)\,\mathrm{d}x}{x-z}. \tag{6}$$

Now let

$$I_1 = \int_{-1}^{-k} \frac{(k+t)\,\mathrm{d}t}{\sqrt{1-t^2}(t-x)} \quad \text{and} \quad I_2 = \int_{k}^{1} \frac{(t-k)\,\mathrm{d}t}{\sqrt{1-t^2}(t-x)} \tag{7}$$

so that

$$\Phi(z) = -K\frac{1-\mathrm{i}f}{2\pi\mathrm{i}} I, \tag{8}$$

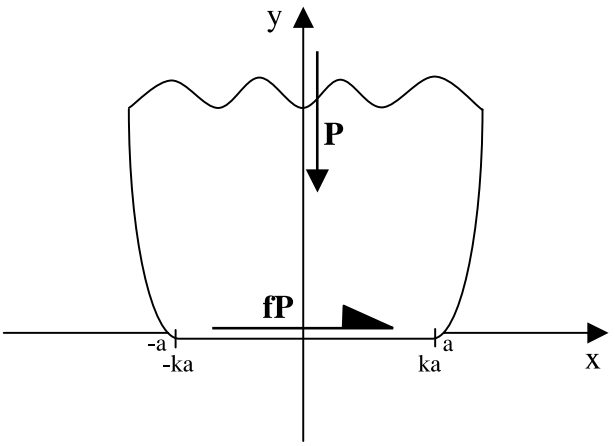

Fig. 3. Representation of a flat punch with rounded edges resting on an elastically similar half plane.

where

$$I = \int_{-1}^{1} \frac{\sqrt{1-x^2}}{x-z}(I_1 + I_2)\,\mathrm{d}x, \equiv I_3 + I_4. \tag{9}$$

A direct approach, solving the inner integrals first, rapidly becomes intractable. However, by changing the order of integration progress can be made. Consider first I_4, changing the order of integration and using partial fractions we obtain

$$I_4 = \int_k^1 \frac{(t-k)}{\sqrt{1-t^2}} \left\{ \int_{-1}^{1} \frac{\sqrt{1-x^2}}{(x-z)(t-x)}\,\mathrm{d}x \right\} \mathrm{d}t, \tag{10}$$

followed by

$$I_4 = \int_k^1 \frac{(t-k)}{\sqrt{1-t^2}} \frac{1}{t-z} \left\{ \int_{-1}^{1} \frac{\sqrt{1-x^2}}{x-z}\,\mathrm{d}x + \int_{-1}^{1} \frac{\sqrt{1-x^2}}{t-x}\,\mathrm{d}x \right\} \mathrm{d}t. \tag{11}$$

The first of the inner integrals is regular whilst the second is a Cauchy principal value, and may be evaluated in closed form to give

$$I_4 = \pi \int_k^1 \frac{(t-k)}{\sqrt{1-t^2}(t-z)} \{R_1 + t\}\,\mathrm{d}t, \tag{12}$$

where $R_1 = \sqrt{z^2-1} - z$. We now note that the fraction in the integrand may be re-written as

$$\frac{(t-k)(R_1+t)}{t-z} = \left(\sqrt{z^2-1} - k\right) + t + \frac{\sqrt{z^2-1}(z-k)}{t-z} \tag{13}$$

which then leaves three integrals which can be evaluated in closed form, to give

$$I_4 = \pi\left[\left(\sqrt{z^2-1} - k\right)\left(\frac{\pi}{2} - \sin^{-1}(k)\right) + \sqrt{1-k^2} + (z-k)\left(\mathrm{i}T(k) - \frac{\pi}{2}\right)\right], \tag{14}$$

where,

$$T(k) = \frac{1}{2}\ln\left[\frac{\mathrm{i}\sqrt{z^2-1}\sqrt{1-k^2} + kz - 1}{\mathrm{i}\sqrt{z^2-1}\sqrt{1-k^2} - kz + 1}\right]. \tag{15}$$

The whole process may be repeated for I_3, to give

$$I_3 = \pi\left[\left(\sqrt{z^2-1} + k\right)\left(\frac{\pi}{2} - \sin^{-1}(k)\right) + (z+k)\left(-\mathrm{i}T(-k) - \frac{\pi}{2}\right)\right]. \tag{16}$$

Finally, therefore,

$$\Phi(z) = -K\frac{1-\mathrm{i}f}{2\mathrm{i}}\left[2\sqrt{z^2-1}\left(\frac{\pi}{2} - \sin^{-1}(k)\right) - \pi z - \mathrm{i}(z+k)T(-k) + \mathrm{i}(z-k)T(k)\right]. \tag{17}$$

Note that if $k = 0$ (the Hertzian contact problem) then $T(-k) = T(k)$ and

$$\Phi(z) = -K\frac{1-\mathrm{i}f}{2\mathrm{i}}\pi R_1 \tag{18}$$

which is correct! We cannot conduct a similar test for $k = 1$ (the square-ended punch) as the pressure has been calculated on the basis of $p(\pm 1) \to 0$ which would not apply if this limit were taken. Fig. 4(a) shows a typical distribution of the normalised von Mises' parameter, $a\sqrt{J_2}/P$, when $k = 0.9$ and $f = 0.6$.

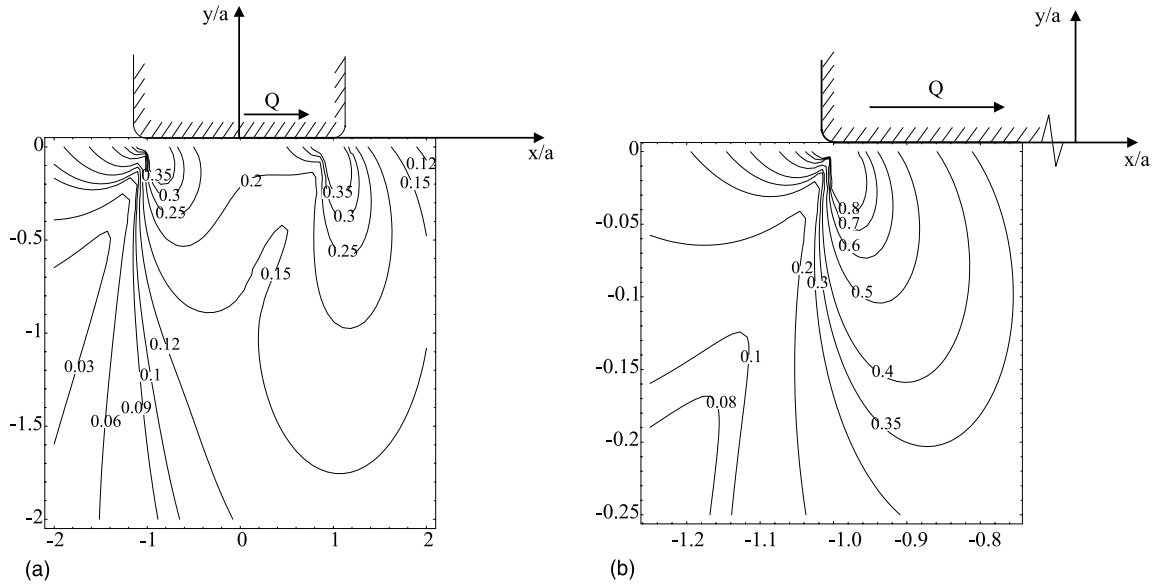

Fig. 4. A typical distribution of the normalised von Mises' parameter, $a\sqrt{J_2}/P$, for a flat pad with rounded edges when $k = 0.9$ and $f = 0.6$ (a) and at the contact edge of a flat pad with rounded edges when $k = 0.9995$ and $f = 0.6$ (b).

Just as we used the semi-infinite punch solution to characterise the stress state at the edge of the finite punch, we can now determine the local stress distribution at the edge of the flat-and-rounded punch. Note that, in practice, we are interested in the state of stress very local to the contact corner, and for values of k close to unity, i.e. where the punch is almost square-ended. This asymptotic solution may be developed following two basic approaches; (a) first, let $k = \sqrt{1 - s^2}$ so that as $s \to 0$, $k \to 1$. Make this substitution into Eq. (17) above, and write the resulting expression as a series expansion in s leading to

$$\Phi(z) = -\frac{3P}{2\pi s^3}\left(\frac{1 - \mathrm{i}f}{2\mathrm{i}}\right)\left(\frac{-2s^3}{3\sqrt{z^2 - 1}} + \mathrm{O}(s^5)\right) \quad s \ll 1 \text{ and } \forall z. \tag{19}$$

We then make the substitution $\eta = z + 1$ followed by $\eta = \rho \mathrm{e}^{\mathrm{i}\theta}$ and use the binomial theorem to simplify the square-root discriminant, with the result

$$\Phi(\eta) \simeq -\frac{P}{\pi}\left(\frac{1 - \mathrm{i}f}{2\sqrt{2\rho}}\right)\exp(-\mathrm{i}\theta/2) \quad s \ll 1 \text{ and } \rho \ll 1. \tag{20}$$

Alternative (b) is to make the substitution $\eta = z + 1$ into Eq. (17) *first*, so that when $\eta \ll 1$ a binomial expansion leads to

$$\Phi(\eta) \simeq -K\frac{1 - \mathrm{i}f}{\sqrt{2}}((\pi - 2\sin^{-1}(k))\sqrt{\rho}\exp(\mathrm{i}\theta/2)), \quad \text{for } \rho \ll 1 \text{ and } \forall k. \tag{21}$$

Comparing the asymptotic solutions presented in Eqs. (20) and (21) we note that: the former results in a square-root singularity and the latter, a bounded solution, as $\rho \to 0$. This is to be expected since the former leads to a square-ended punch as $k \to 1$. The latter expression holds for any k, where we know that the solution is bounded. In the present investigation, Eq. (17) was employed to investigate the local stress state at the contact edge, and Fig. 4(b) shows an example distribution of $a\sqrt{J_2}/P$ for $k = 0.9995$ and $f = 0.6$.

4. The effect of edge radii

If the punch under consideration has a finite corner radius, then it must be the case that the traction components of stress vanish as the edge is approached, and hence, from Way's theorem (Way, 1940), so must the other stress components, at least under frictionless conditions. It follows that, formally, the state of stress in the neighbourhood of the contact edge can never be properly represented by the asymptotic solution of a square-ended semi-infinite punch which is, by definition, square-root singular. On the other hand, a simple comparison of the contact pressure distributions adjacent to, but not at the contact edge (Navarro et al., submitted for publication), shows that the latter may be scaled so that it fits the pressure distribution of a flat-and-rounded punch over a wide region, providing that k is very close to unity.

A comparison is needed between the full field solution for a flat-and-rounded punch, and the semi-infinite square-ended punch solution. This may easily be achieved through the medium of the finite square-ended flat punch; the flat square-ended and flat-and-rounded punch solutions may be compared simply by using the same contact load, i.e. keeping $ap(x)/P$ the same for each. The semi-infinite punch solution is then abstracted from the former in the manner described above.

5. Asymptotic solution

It is instructive, first, to examine the domain of validity of the semi-infinite punch solution as a representation of the finite square-ended punch solution, as this requires no scaling, and formally approaches the finite flat punch solution as the corner is approached. We note from Fig. 2(b) that the lines of constant discrepancy run slanted to the right with the contour of 'zero' error passing through the point (0,0), as expected. Above and to the right of this contour, the full field is stronger (higher order terms becoming significant), while below, it is weaker than the solution implied by the semi-infinite punch.

A comparison between the full field of the flat-and-rounded punch and the asymptotic solution implied by the semi-infinite punch was made next. Practical cases of interest are when k is very close to unity, and the example results shown in Figs. 5 and 6 are for $k = 0.9991$ and 0.9999, respectively, for $f = 0.6$. Each figure displays two basic sets of contours:

1. Contours of constant discrepancy, $(a\sqrt{J_2}_{\text{full}}/P - a\sqrt{J_2}_{\text{asymp}}/P)/a\sqrt{J_2}_{\text{full}}/P$, between the respective magnitudes of the normalised von Mises' yield parameter.
2. Contours representing the shape and size of the local crack initiation environment, or process zone, as measured by the von Mises' yield criterion, $\sqrt{J_2}$, based on the flat-and-rounded punch full field solution. The plastic front is shown as a function of $P/a\tau_y$, where τ_y is the yield stress in pure shear.

Each set of contours is displayed on two different scales, one very close to, and the other slightly further from the contact edge. The reasons behind this will become clearer as the solution is developed. The object of the second set of contours is to display the range of process or plastic zone sizes which may be characterised by the singular solution, employed as an idealisation of the actual plastic zone given by the full field solution. It is assumed that small scale yielding principles apply, so that yielding is quantified by using the elasticity solution to the problem, and finding out where the yield criterion is exceeded, in the spirit of the standard plastic zone calculations carried out at crack tips in LEFM. The process zone is controlled by an elastic hinterland, so that the region of matching of the asymptotic solution (to within an arbitrary specified tolerance) must extend 'well beyond' the process zone itself.

It is important to recognise that the full flat-and-rounded punch field and the asymptotic field match exactly only along a particular contour $\rho(\phi)$. The two fields diverge for larger values of ρ in a similar sense to the divergence between the full square-ended punch and semi-infinite punch solutions. However, they

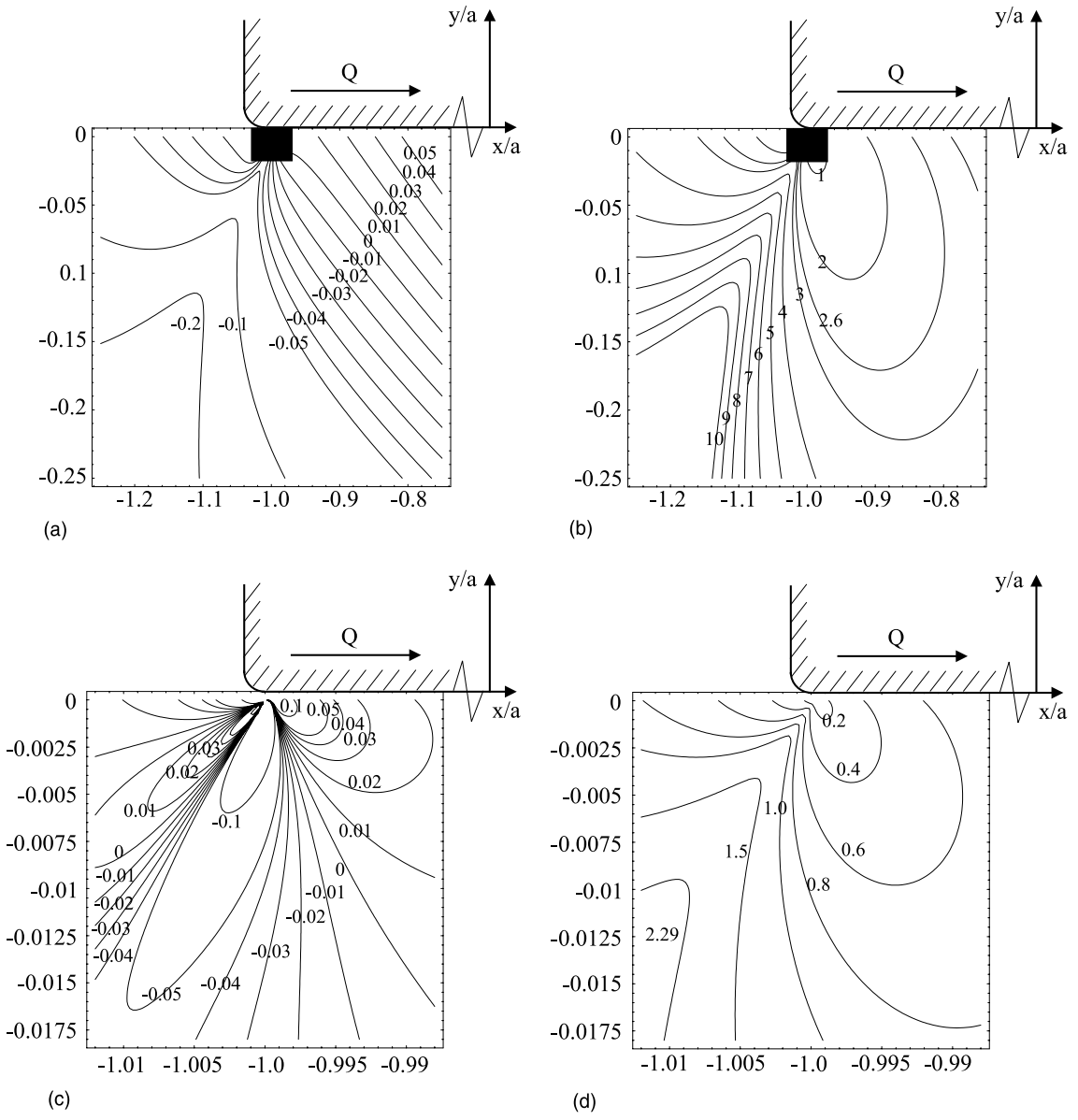

Fig. 5. (a) Plot showing the "outer boundary" discrepancy between the flat-and-rounded full field solution and the asymptotic semi-infinite punch solution, $(a\sqrt{J_{2\text{full}}}/P - a\sqrt{J_{2\text{asymp}}}/P)/a\sqrt{J_{2\text{full}}}/P$, when $k = 0.9991$ and $f = 0.6$. (b) Plot showing the "outer boundary" plastic yield fronts, $P/a\tau_y$, when $k = 0.9991$ and $f = 0.6$. (c) Plot showing the "inner boundary" discrepancy between the flat-and-rounded full field solution and the asymptotic semi-infinite punch solution, $(a\sqrt{J_{2\text{full}}}/P - a\sqrt{J_{2\text{asymp}}}/P)/a\sqrt{J_{2\text{full}}}/P$, when $k = 0.9991$ and $f = 0.6$. (d) Plot showing the "inner boundary" plastic yield fronts, $P/a\tau_y$, when $k = 0.9991$ and $f = 0.6$.

also diverge for small values of ρ, because the two fields are qualitatively very different as $\rho \to 0$. The outer limit of the zone of approximate matching is well outside the region in which the stress field has a steep gradient, in the neighbourhood of the flat-to-rounded transition. In the conventional application of an asymptotic solution (in the sense of a classical crack problem or the finite square-ended punch problem),

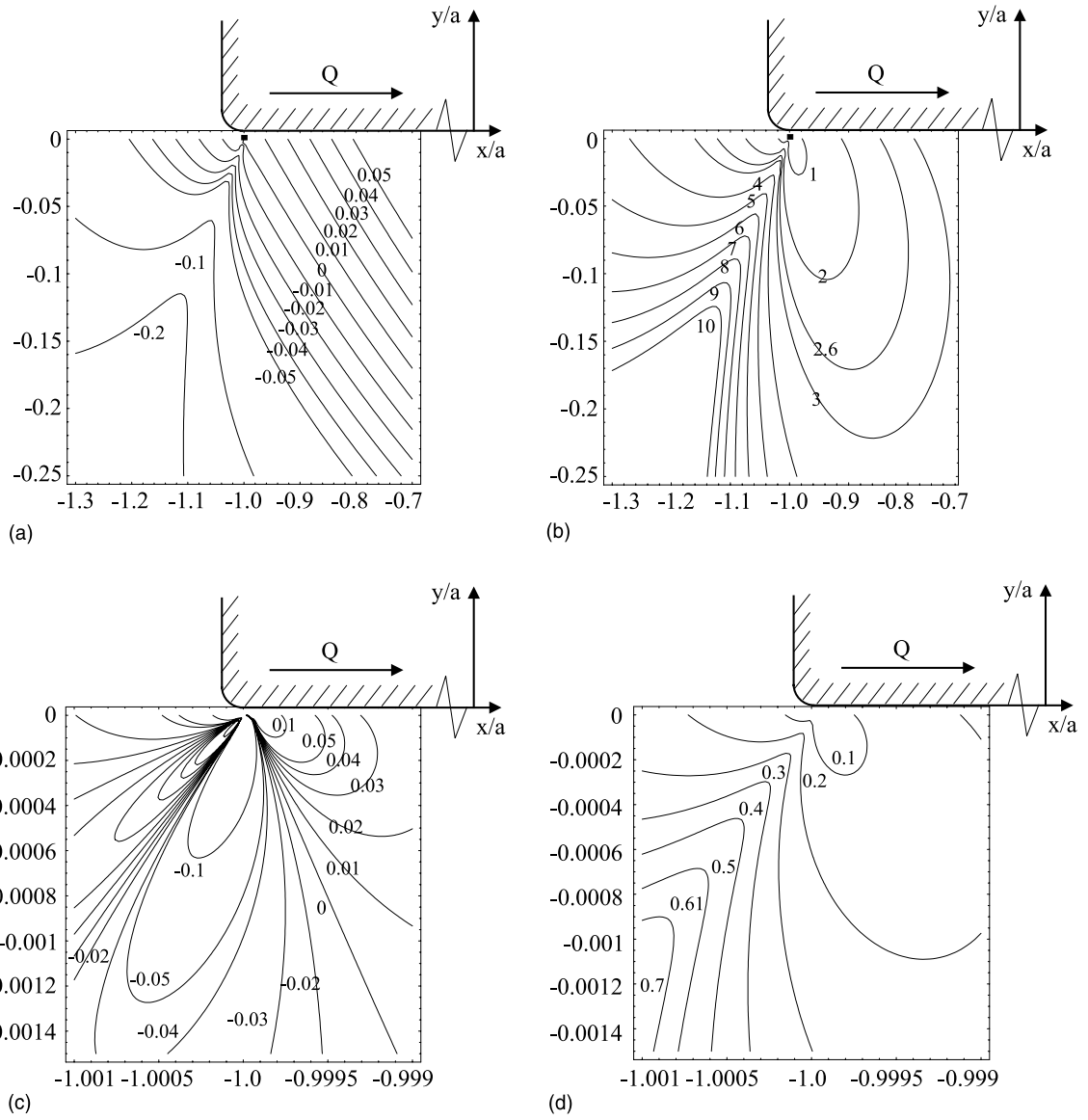

Fig. 6. (a) Plot showing the "outer boundary" discrepancy between the flat-and-rounded full field solution and the asymptotic semi-infinite punch solution, $(a\sqrt{J_{2\text{full}}}/P - a\sqrt{J_{2\text{asymp}}}/P)/a\sqrt{J_{2\text{full}}}/P$, when $k = 0.9999$ and $f = 0.6$. (b) Plot showing the "outer boundary" plastic yield fronts, $P/a\tau_y$, when $k = 0.9999$ and $f = 0.6$. (c) Plot showing the "inner boundary" discrepancy between the flat-and-rounded full field solution and the asymptotic semi-infinite punch solution, $(a\sqrt{J_{2\text{full}}}/P - a\sqrt{J_{2\text{asymp}}}/P)/a\sqrt{J_{2\text{full}}}/P$, when $k = 0.9999$ and $f = 0.6$. (d) Plot showing the "inner boundary" plastic yield fronts, $P/a\tau_y$, when $k = 0.9999$ and $f = 0.6$.

there is only an upper bound on the magnitude of the acceptable load. This is because the discrepancy between the asymptotic and full field solutions decreases monotonically as ρ decreases. When comparing the flat-and-rounded punch and semi-infinite solutions, there is also a *minimum* load which can be tolerated, because of the divergence of the two solutions for small ρ. It is precisely this behaviour that leads us to display the above two sets of contours on two different length scales. Figs. 5 and 6 display these load

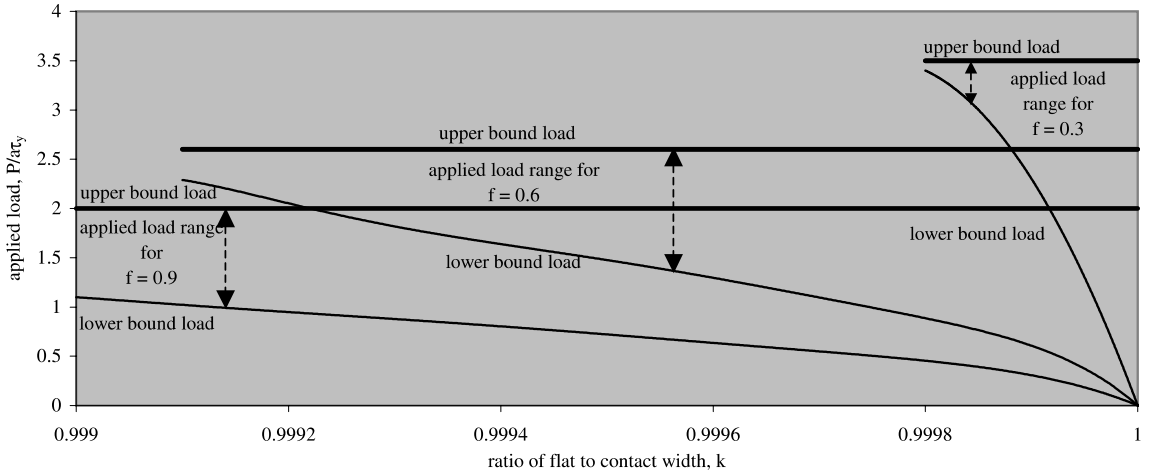

Fig. 7. Plot showing the upper and lower bounds of the applied load, $P/a\tau_y$, as a function of k such that the maximum discrepancy is 5% for $f = 0.3$, 0.6 and 0.9.

boundaries under specific conditions where the tolerable discrepancy between the full and asymptotic solutions *at the plastic boundary*, has been arbitrarily set at 5%; looking at Fig. 5(a) and (b), ($k = 0.9991$ and $f = 0.6$) the upper load boundary, we see that $P/a\tau_y$ is about 2.6. From Fig. 5(c) and (d), the lower load boundary, $P/a\tau_y$, is about 2.29. For the case of $k = 0.9999$ and $f = 0.6$, Fig. 6, the load boundaries are given as $0.61 \leqslant P/a\tau_y \leqslant 2.6$. Many plots of this kind were obtained, and from them the range of acceptable normalised loads, $P/a\tau_y$, were found. Thus, the load range is known as a function of the proximity of the local elastic stress state to the square-ended punch solution. This information is summarised in Fig. 7 for three sample coefficients of friction, viz. 0.3, 0.6 and 0.9, and is an intermediate form of the results used to find the load range for a particular geometry.

From Fig. 7 we note that the upper bound on the contact load is, for practical purposes, independent of the value of k, precisely because the physical location of the plastic front at the upper bound load is well removed from the location of the steep pressure gradient, itself a strong function of k. Conversely, the lower bound load is strongly dependent on the value of k; it decreases with increasing k (at a steeper gradient for smaller f) so that when $k \equiv 1$ it vanishes leaving only an upper bound load. Additionally, with a decreasing value of k the lower bound load approaches the upper bound load until the two coincide. The point at which they converge is friction dependent taking place at smaller values of k for larger f. At still smaller values of k there is no valid solution.

6. Application of results

In a real problem the value of the contact patch semi-width, a, is not known, but is a dependent variable of the calculation, whereas the length of the flat portion of the punch, $2ka$, is known; neither k nor a is known individually. If we let the product, ka, be denoted by b, the contact law defined as

$$\frac{PR}{E^* b^2} = \frac{\pi - 2\phi_0}{4\sin^2\phi_0} - \frac{\cot\phi_0}{2}, \qquad \phi_0 = \sin^{-1} b/a \tag{22}$$

may be used to eliminate "a" from the expressions defining the normalised von Mises' parameter, $a\sqrt{J_2}/P$, leading to the dimensionless quantity, $R\tau_y/E^*b$.

In practical problems, the quantities which are normally known are; the length of the flat portion of the punch ($2b$), the material properties (E^*, τ_y), the applied load, P, and the punch corner radius, R. The acceptable range of values of P is what is needed, and k becomes an intermediate parameter in the calculation. This information may be obtained directly from Figs. 8–10 for three sample coefficients of friction, 0.3, 0.6 and 0.9, respectively. These display the acceptable dimensionless load range, $P/b\tau_y$, to ensure no more than a 5% discrepancy between the actual elastic stress state and that given by the semi-infinite square-ended punch solution. This condition is imposed at the implied elastic-plastic boundaries, as a function of the dimensionless edge radius, $R\tau_y/E^*b$. Fig. 11 combines these plots for ease of comparison, but omits the contours of the intermediate variable, k, for clarity.

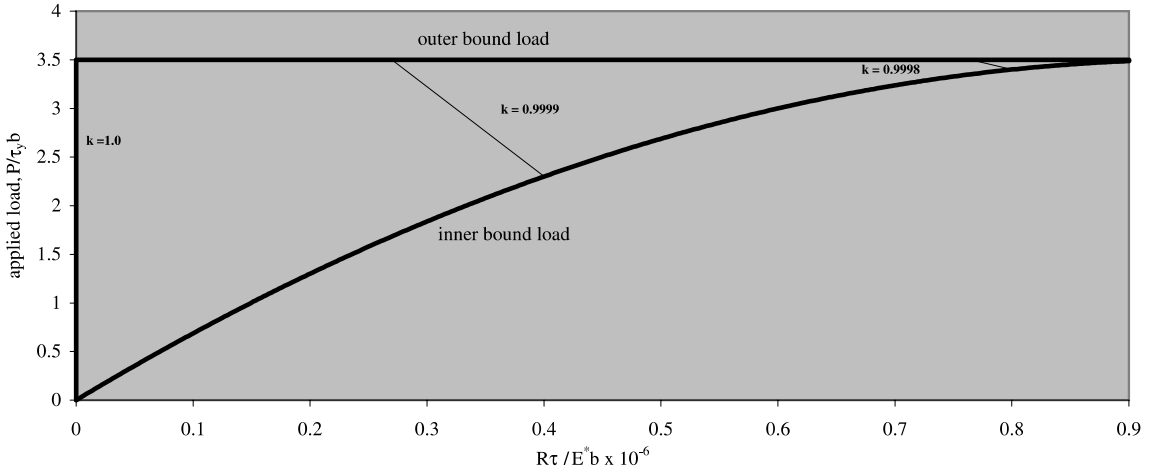

Fig. 8. Plot of the applied load, $P/b\tau_y$, against $R\tau_y/E^*b$, showing the region over which the maximum discrepancy between the asymptotic and full field solutions is 5% for contours of constant k when $f = 0.3$.

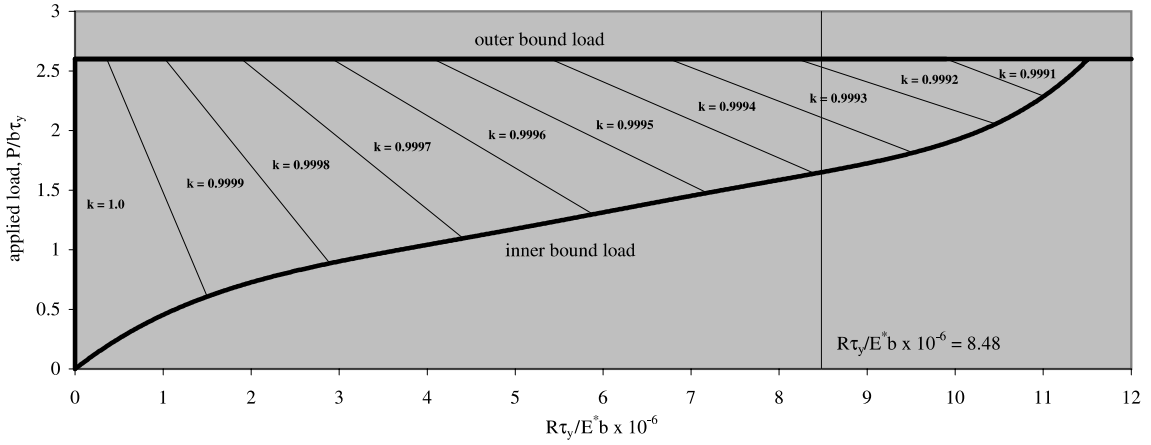

Fig. 9. Plot of the applied load, $P/b\tau_y$, against $R\tau_y/E^*b$, showing the region over which the maximum discrepancy between the asymptotic and full field solutions is 5% for contours of constant k when $f = 0.6$.

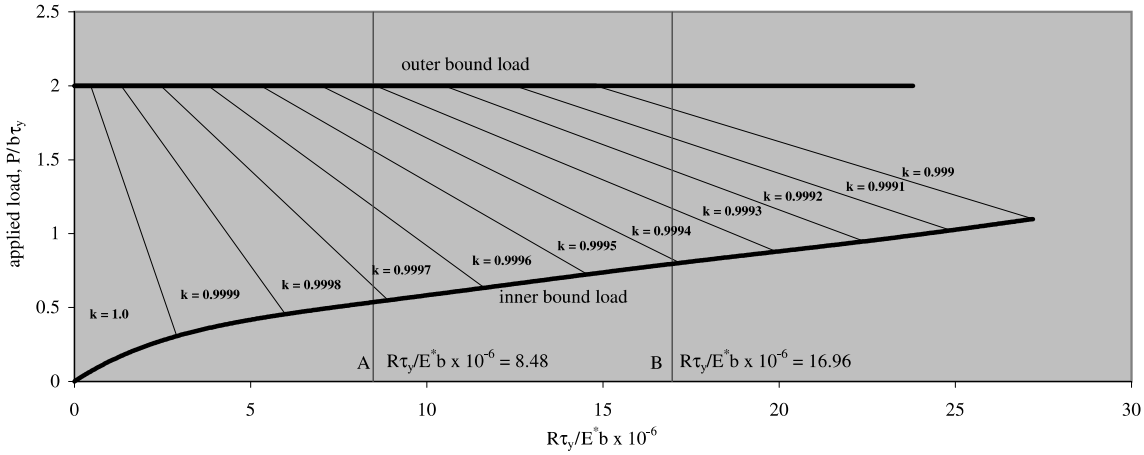

Fig. 10. Plot of the applied load, $P/b\tau_y$, against $R\tau_y/E^*b$, showing the region over which the maximum discrepancy between the asymptotic and full field solutions is 5% for contours of constant k when $f = 0.9$.

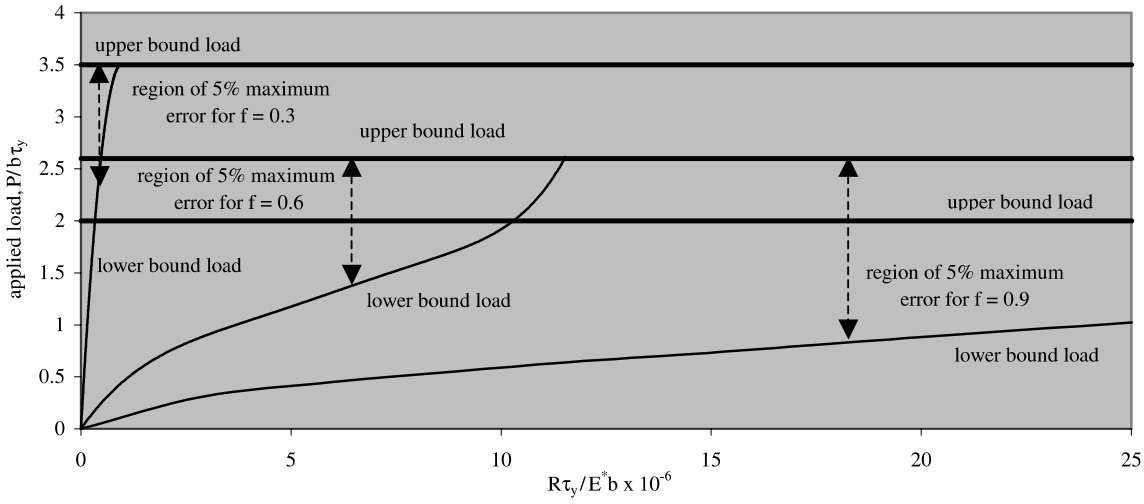

Fig. 11. Plot of the applied load, $P/b\tau_y$, against $R\tau_y/E^*b$, showing the region over which the maximum discrepancy between the full and asymptotic fields is 5% for various coefficients of friction.

Before proceeding to determine that range of acceptable applied loads, we note three observations from Fig. 11; (a) a wide range of R values can be tolerated in relation to the upper bound load on the plastic zone size, (b) the lower bound load which can be tolerated is strongly dependent on R; it becomes vanishingly small as $R \to 0$ but coincides with the upper bound load at specific values of k and f. Lastly, (c) the tolerable R value range (corresponding to the lower bound load) increases with increasing coefficient of friction; it is quite extensive when f is 0.9, but very restricted indeed when f is 0.3. Thus, for a coefficient of friction of 0.6, Fig. 9, there is no acceptable load range where the asymptotic solution applies if $R\tau_y/E^*b > 11.5 \times 10^{-6}$.

As a practical example, consider the case of a nominally flat pad with $b = 5$ mm. Assume that the material has an elastic constant E^* of 112 kN/mm^2, a yield strength in shear, τ_y, of 475 N/mm^2, and that the

coefficient of friction is 0.6. If the pad radius were 10 μm then $R\tau_y/E^*b = 8.48 \times 10^{-6}$ (depicted in Fig. 9 as the vertical dashed line running through this point). In order to determine the load range we note the points at which the dashed line crosses the inner and outer load bound curves, so that the load range is given as $1.65 < P/b\tau_y < 2.6$ which corresponds to $3919 < P\ (\mathrm{N/mm}) < 6175$. If instead f was 0.9 (Fig. 10, curve A), the applied load range would be given by $1259 < P\ (\mathrm{N/mm}) < 4750$, while for the same coefficient of friction and $R = 20$ μm (Fig. 10, curve B), the load range is $1900 < P\ (\mathrm{N/mm}) < 4750$. Note that in the case of $f = 0.3$, R would have to be of the order 0.5 μm in order for matching within the specified tolerance to be achieved, i.e. $R\tau_y/E^*b = 0.8 \times 10^{-6}$.

7. Conclusion

The asymptotic solution of a semi-infinite, square-ended punch, has been extracted from the known Muskhelishvili potential for a finite, square-ended rigid punch, sliding against an incompressible half-plane. A closed form solution of the Muskhelishvili potential for a flat punch with rounded edges sliding against an elastically similar half-plane has been used to define the stress state everywhere in the half plane. The asymptotic solution was then compared to the full field solution of the flat-and-rounded configuration, at the contact edge. This comparison reveals two boundaries: an inner and outer boundary, such that the assumptions of small-scale yielding might be invoked for a specified discrepancy between the two solutions. This involved determining the shape and size of the plastic fronts, based on the elasticity solution, so that the maximum allowable discrepancy was not exceeded. We therefore determined an upper and lower bound load which are functions of the coefficient of friction, f, and the ratio of the flat to contact width, k. It has been shown that for a given f the upper load bound is practically independent of k while the lower load bound is strongly dependent on k.

We go on to define a dimensionless parameter, $R\tau_y/E^*b$, based on physically measurable variables, and obtain contours such that the upper and lower discrepancy bounds are not exceeded. This is then plotted against the applied load, $P/b\tau_y$, resulting in a region over which matching to within the specified tolerable discrepancy is achieved. It is then possible to determine the range of P values (for given R values) such that the assumptions of small-scale yielding hold. Conversely, the analysis shows that the range of acceptable R values increases with the coefficient of friction, and that although in the manufacture of a nominally square-ended complete contact, a finite edge radius will arise, under certain conditions the practically acceptable values of R lie within manufacturing tolerances. However, in situations where the value of k is rather smaller such as in the dovetail joints used in gas turbines, the same conclusion cannot be drawn.

It should also be emphasized that the whole calculation was carried out on the basis of a *sliding* contact, in order to reduce the number of dependent variables. An extension to partial slip would clearly be possible and straightforward.

References

Ciavarella, M., Hills, D.A., Monno, G., 1998. The influence of rounded edges on indentation by a flat punch. Proc. Instn. Mech. Engrs. 212 C, 319–328.

Comninou, M., 1976. Stress singularity at a sharp edge in contact problems with friction. J. Appl. Math. Phys. (ZAMP) 27, 493–499.

Gdoutos, E.E., Theocaris, P.S., 1975. Stress concentration at the apex of a plane indenter acting on an elastic half plane. J. Appl. Mech. 42, 688–692.

Giannakopoulos, A.E., Lindley, T.C., Suresh, S., 1998. Aspects of equivalence between contact mechanics and fracture mechanics: theoretical connections and a life-prediction methodology for fretting-fatigue. Acta Mater. 46, 2955–2968.

Hills, D.A., Nowell, D., Sackfield, A., 1993. Mechanics of Elastic Contact. Butterworth, Heinemann, Oxford, UK.

Jäger, J., 2002. New analytical and numerical results for two-dimensional contact profiles. Int. J. Solids Struct. 39, 959–972.

Mugadu, A., Hills, D.A., 2002. A generalised stress intensity approach to characterising the process zone in complete fretting contacts. Int. J. Solids Struct. 39, 1327–1335.

Mugadu, A., Hills, D.A., Limmer, L., 2002. An asymptotic approach to crack initiation in fretting fatigue of complete contacts. J. Mech. Phys. Solids. 50, 531–547.

Navarro, C., Hills, D.A., Dominguez, J., submitted for publication. The effect of corner radius on an asymptotic solution to the fretting of complete contacts. Fat. Fract. Engng. Mat. Struct.

Way, S., 1940. Some observations on the theory of contact pressures. J. Appl. Mech. 7, 147–157.